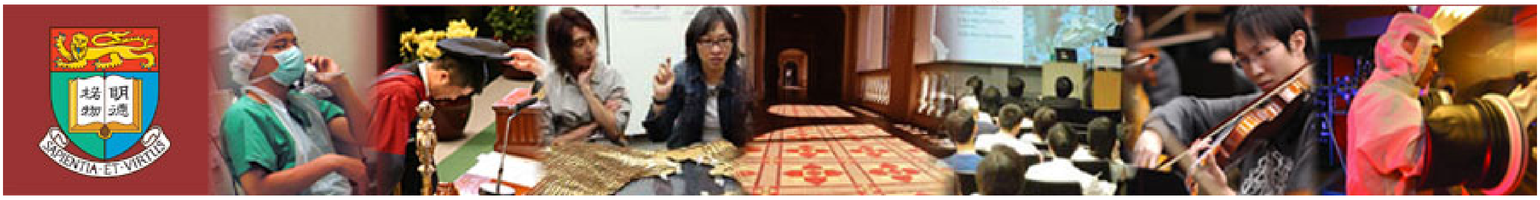

Title	El Niño Modulations Over The Past Seven Centuries (Letter to the editor)
Author(s)	Li, J; Xie, S-P; Cook, ER; Morales, MS; Christie, D; Johnson, N; Chen, F; D'Arrigo, R; Fowler, A; Gou, X; Fang, K
Citation	Nature Climate Change, 2013, v. 3 n. 9, p. 822-826
Issued Date	2013
URL	http://hdl.handle.net/10722/189524
Rights	Creative Commons: Attribution 3.0 Hong Kong License

El Niño modulations over the past seven centuries

Jinbao Li[1,2*], Shang-Ping Xie[2,3,4], Edward R. Cook[5], Mariano S. Morales[6], Duncan A. Christie[7,8], Nathaniel C. Johnson[2], Fahu Chen[9], Rosanne D'Arrigo[5], Anthony M. Fowler[10], Xiaohua Gou[9] and Keyan Fang[9]

[1]Department of Geography, University of Hong Kong, Hong Kong.

[2]International Pacific Research Center, University of Hawaii at Manoa, Honolulu, HI 96815, USA.

[3]Scripps Institution of Oceanography, University of California at San Diego, La Jolla, CA 92093-0230, USA.

[4]Physical Oceanography Laboratory and Ocean–Atmosphere Interaction and Climate Laboratory, Ocean University of China, Qingdao 266100, China.

[5]Lamont-Doherty Earth Observatory, Columbia University, Palisades, NY 10964, USA.

[6]Instituto Argentino de Nivología, Glaciología y Ciencias Ambientales (IANIGLA), CCT-CONICET, C.C. 330, 5500 Mendoza, Argentina.

[7]Laboratorio de Dendrocronología y Cambio Global, Instituto de Conservación Biodiversidad y Territorio, Facultad de Ciencias Forestales y Recursos Naturales, Universidad Austral de Chile, Casilla 567, Valdivia, Chile.

[8]Center for Climate and Resilience Research [CR]^2, Chile.

[9]MOE Key Laboratory of Western China's Environmental System, Lanzhou University, Lanzhou 730000, China.

[10]School of Environment, The University of Auckland, Auckland 1020, New Zealand.

*E-mail: jinbao@hku.hk

Predicting how El Niño/Southern Oscillation (ENSO) will change with global warming is of enormous importance to society[1-4]. ENSO exhibits considerable natural variability at interdecadal-centennial time scales[5]. Instrumental records are too short to determine whether ENSO has changed[6] while existing reconstructions are often developed without adequate tropical records. Here we present a seven-century long ENSO reconstruction based on 2222 tree-ring chronologies from both the tropics and mid-latitudes in both hemispheres. The inclusion of tropical records enables us to achieve unprecedented accuracy, as attested by high correlations with equatorial Pacific corals[7,8] and coherent modulation of global teleconnections that are consistent with an independent Northern Hemisphere temperature reconstruction[9]. Our data indicate that ENSO activity in the late twentieth century was anomalously high over the past seven centuries, suggestive of a response to ongoing global warming. Climate models disagree on the ENSO response to global warming[3,4], suggesting that many models underestimate the sensitivity to radiative perturbations. Illustrating the radiative effect, our reconstruction reveals robust ENSO response to large tropical eruptions, with anomalous cooling in the east-central tropical Pacific in the year of eruption, followed by anomalous warming one year after. Our observations provide crucial constraints for improving climate models and their future projections.

El Niño and La Niña are the warm and cold phases of the El Niño/Southern Oscillation (ENSO) cycle, and have profound impacts on worldwide weather and climate through large-scale, far-reaching patterns known as atmospheric teleconnections[1,2]. State-of-the-art climate models disagree on the nature of ENSO behavior in a warmer climate[3,4].

ENSO properties, such as amplitude, frequency, and associated teleconnection patterns, have undergone considerable natural variability at interdecadal (10-90 years) to centennial (~100 years) time scales[5,10]. Instrumental records, available for only about the past 150 years, are not nearly long enough to capture the full behavior of ENSO variability[6]. Multiple paleo-reconstructions of ENSO activity are available (Supplementary Table S1), but they generally cover the past few centuries or noncontinuous fractions of the past millennium, and many of them do not represent ENSO variability directly, due to their strong dependence on extratropical proxy records. To address these challenges, we compile and synthesize 2222 tree-ring chronologies from both the tropics and mid-latitudes of both hemispheres to reconstruct ENSO variability for the past seven centuries. By consolidating coherent signals in tree-rings from such diverse regions, we aim to represent ENSO variability more accurately.

Our tree-ring network is composed of 2222 chronologies from Asia, New Zealand, and North and South America (Supplementary Table S2). Of these, strong ENSO signals are found in tree rings from seven regions, including two in the tropics (Maritime Continent and South American Altiplano), three in the mid-latitude Northern Hemisphere (Central Asia, Southwest North America, and the Pacific Northwest/Texas-Mexico (TexMex) region), and two in the mid-latitude Southern Hemisphere (northern New Zealand and west-central Argentina) (Fig. 1a). We extract regional variability from tree rings by either a principal components analysis or the development of a regional chronology (Supplementary Methods). The resultant seven time series, one from each region, serve as the basis for our ENSO reconstruction. The first principal component (PC1) of the seven time series, covering the period 1301-1992 and explaining 26.6% of the total variance, is highly correlated with tropical Pacific sea surface temperatures[11] (SSTs; Fig. 1a). PC1 correlates highly with the prior November-January (NDJ) Niño3.4 index ($r = 0.80$) during 1871-1992. The correlation with the Trans-Niño Index[12], a measure of the zonal SST gradient, is statistically significant but much lower ($r = -0.43$), suggesting that the tree rings are most sensitive to east-central tropical Pacific SST anomalies instead of their east-west gradient. Therefore, we develop a reconstruction for the canonical ENSO variability (Methods and Supplementary Fig. S1), as represented by the Niño3.4 index (Fig. 1b).

Our reconstruction is highly correlated with existing ENSO records, whether their input data are completely independent or with a few overlapping subsets (Supplementary Table S1). Compared with other reconstructions, ours incorporates tree rings from two tropical regions that have higher weights in the Empirical Orthogonal Function (EOF) than the extratropical peers (Supplementary Table S2), leading to a roughly 10% increase in explained instrumental ENSO variance (Supplementary Table S1). To further verify the reconstruction, we compare it with independent records from the equatorial Pacific: (1) The Southern Oscillation Index[13] (SOI) is a standardized index of sea level pressure difference between Tahiti and Darwin, Australia (Fig. 1a), and represents the atmospheric component of ENSO. Our reconstruction correlates at -0.67 ($p < 0.001$) with the boreal winter (September-February) SOI for their common period 1867-2005 (Fig. 1c), close to the correlation between instrumental Niño3.4 SST and SOI indices for the same period ($r = -0.83$). (2) Our reconstruction is significantly correlated with modern coral records in the central tropical Pacific: $r = -0.57$ ($p < 0.001$) at Maiana Atoll[7] for 1841-1994 (Fig. 1d), and $r = -0.53$ ($p < 0.001$) at Palmyra Island[8] for 1887-1998 (Fig. 1e). After adjusting relict coral U/Th dates within the analytical error windows[5], we find that significant correlations between our reconstruction and Palmyra corals have persisted throughout the past seven centuries (Fig. 1e). The above agreements are remarkable in that these proxy records are completely independent, indicating high fidelity of our reconstruction over the past seven centuries.

The reconstructed ENSO index displays marked variations at interannual to interdecadal time scales over the past seven centuries (Fig. 1f). The multi-taper method[14] (MTM) spectral analysis reveals that significant ENSO periodicities fall within interannual (2-7 years) and decadal (8-13 years) bands, respectively (Supplementary Fig. S2a). The interannual cycles are observed for the instrumental era, a period when the decadal cycles are less pronounced (Supplementary Fig. S3). The time-space wavelet analysis[15] shows that the interannual variability has persisted throughout the past seven centuries, while the decadal variability weakens during most of the sixteenth and twentieth century (Supplementary Fig. S2b). Marked decadal variability is also widely found in Indo-Pacific corals in the late nineteenth century, with its spatial pattern closely resembling that of interannual variability[16]. Together these results suggest that decadal variability is a significant component of ENSO system and is underestimated by instrumental data. We have investigated the relationship between the decadal variability and sunspot number using a cross-wavelet transform (Supplementary Methods). There is a strong spectral coherence but the phase varies by 180º over the course of their common period (Supplementary Fig. S4). If the 11-year solar cycle is linked to decadal ENSO variability, then the mechanism must be able to accommodate meandering 180º phase reversals through time, and has not yet been determined through climate modeling studies.

Instead, decadal ENSO variability more likely results from internal dynamics.

Temporal evolution of ENSO variance represented by our reconstruction is most consistent with that shown by the two tropical records (Supplementary Fig. S5). The mutual agreement between the two independent tropical records suggests that our reconstruction represents ENSO variance more accurately than previous ones that generally do not incorporate tropical records. Overall the reconstructed ENSO variance was weak in the early Little Ice Age (LIA) of 1300s-1550s, increased during the late LIA of 1550s-1880s, and became unusually high after the 1880s (Fig. 2a). The reconstruction also exhibits larger variance than the instrumental target in the early twentieth century. The empirical reconstructions may underestimate SST variability due to the lack of observations in that period[2].

The reconstructed ENSO variance exhibits substantial modulation at interdecadal to centennial time scales (Fig. 2a). Such modulation, however, may arise stochastically and thus may not be indicative of dynamics with intrinsic interdecadal time scales[17,18]. We estimate the expected range of variability of 31-yr running biweight variance that may arise stochastically through a Monte Carlo approach (Supplementary Methods). The results indicate that the interdecadal modulation of ENSO variance before 1900 may arise stochastically (Fig. 2a). Running variance during much of the twentieth century, however, exceeds the 95% confidence interval for stochastic variations, suggesting that the recent enhancement of ENSO variance is due to changes in the background state such as the secular positive trend in tropical SSTs[19]. Climate models disagree on the ENSO response to global warming, splitting between enhanced and damped variability[3,4]. Our observations suggest that models with a damped response may underestimate the sensitivity of ENSO to increasing anthropogenic radiative forcing, although significant ENSO changes may still be difficult to detect for periods of less than a century[6]. Regardless, a more thorough attribution of interdecadal ENSO variability in future work requires the combination of developments in theory, coupled climate model simulations, and long records of ENSO variability like ours.

Determining the strength of ENSO teleconnections is crucial for climate forecasts outside the tropical Pacific. Instrumental records show substantial modulation of ENSO teleconnections on interdecadal time scales during the twentieth century[10, 20], but the cause of such modulation remains unclear. Here we calculate 31-year running correlations between the reconstruction and each input series to assess the stationarity of ENSO teleconnections over the pan-Pacific regions for the past seven centuries. The ENSO influence is most robust over the Maritime Continent (Fig. 2b), perhaps not surprisingly as it is a center of action for ENSO with strong rainfall variability. The ENSO teleconnection is also robust over Central Asia, except for marked reduction within the Maunder minimum of 1660s-1700s (Fig. 2b). Marked reduction in the strength of ENSO teleconnections during the Maunder minimum is also found over the South American Altiplano and northern New Zealand (Fig. 2d), but not over western North America (Fig. 2c). Overall, ENSO teleconnections are robust over the South American Altiplano and Southwest North America for most of the past seven centuries, but vary substantially over northern New Zealand and the Pacific Northwest/TexMex region (Figs. 2c and 2d). Relative to the ENSO variance time series, we find that ENSO teleconnections over the pan-Pacific regions are generally strong (weak) when the ENSO variance is high (low), with each high/low-variance epoch lasting for several decades

(Figs. 2a-2d). Likewise, we find that ENSO teleconnections on Northern Hemisphere (NH) temperature are linked to changes in ENSO variance (Supplementary Methods and Fig. S6). These concomitant changes throughout the past seven centuries indicate that the ENSO effects on extratropical climate are modulated by ENSO variance at interdecadal to centennial time scales.

Explosive volcanic eruptions affect the climate by injecting aerosols into the atmosphere[21], but their effect on ENSO remains uncertain, with inconclusive results from short observations[21-23] and contradictory results from model simulations[24-26]. Here we use Superposed Epoch Analysis[22] (SEA) to assess their relationship for the past seven centuries. We employ a historical/geological record-based Volcanic Explosivity Index[27] (VEI), which more accurately records eruption location than other indices derived from polar ice core chemistry (Supplementary Table S4). Using a series of sensitivity tests, the results indicate a robust ENSO response to large tropical eruptions (VEI > 4; 22 events), but not to medium eruptions (VEI = 4; 68 events) (Supplementary Tables S5). For large tropical eruptions, immediate cooling tends to occur in the east-central tropical Pacific in the year of eruption (t = 0), followed by anomalous warming one year after (Fig. 3a). On average, the Niño3.4 SST difference from year t=0 to year t+1 amounts to ~1.0°C, statistically significant at the 0.01 level, based on a two-tailed student's t-test.

Previous studies using shorter and less reliable ENSO reconstructions yielded only a vague picture of a multi-year warming response to a large tropical eruption[22-25]. Our analysis, based on a longer and more accurate ENSO reconstruction, reveals a much richer evolution. An intermediate climate model simulates the subsequent warming through an ocean dynamical thermostat mechanism[28], but not the initial cooling response[24,25]. A recent study using a fully coupled general circulation model (GCM) suggests a concurrent cooling response to volcanic forcing[26]. Our observations now offer support for the GCM result, suggesting that in addition to the thermostat mechanism, other dynamical processes such as zonal variations in SST damping are important for simulating the full response of ENSO to radiative forcing perturbations.

Did large tropical eruptions cause moisture extremes recorded in tree-rings by direct radiative forcing or through the effects on ENSO? To answer this question, we compare volcanically-induced moisture anomaly patterns to those of ENSO. The close resemblance of moisture pattern at year t=0 (t+1) to that of La Niña (El Niño) provides strong evidence that tropical eruptions affect global moisture largely through the influence on ENSO (Figs. 3b-3e).

In summary, our tree-ring based ENSO reconstruction for the past seven centuries represents a major improvement over previous efforts, made possible by including records from the tropics. Our results show marked interdecadal-centennial variations in ENSO amplitude that modulate its effects on extratropical climate, suggesting that ENSO variance, rather than alternative mechanisms such as mid-latitude waveguide modulation[29], is a primary control of the modulations. On longer time scales, ENSO variance is low in the early LIA period and high in the twentieth century. The elevated ENSO variability in recent decades is unprecedented over the past seven centuries, suggesting a response to increased anthropogenic radiative forcing. Climate models disagree on the response to global warming, suggesting that many of them may underestimate ENSO sensitivity to radiative perturbations. While ENSO is an internal mode of the coupled system, our analysis with a large sample size reveals a robust response to large tropical volcanic eruptions. Large tropical eruptions force the Pacific immediately into an anomalous cooling state, followed by anomalous warming in the next year. The response to the 11-year solar cycle is inconsistent in phase over the record, possibly because of weak forcing. This underlines the complexity of ENSO dynamics and calls for further investigations into the sensitivity to the magnitude and timescale[19] of radiative forcing. Regardless, the robust ENSO response to volcanic forcing, and in particular its evolution in time, offers an excellent test bed for climate models if they are to yield future projections with confidence.

Methods:

We developed an ENSO reconstruction with a well-tested PC regression procedure (see Supplementary Methods). The PC1 of the tree-ring records was retained to build a linear regression model by calibrating on the NDJ Niño3.4 index during 1871-1992. The reconstruction was extended to 2005 with a nested approach, with two iterative regression nests ending in 2003 (six input series) and 2005 (five input series). We performed rigorous calibration and verification tests, and the results indicate significant skill in all three regression models (Supplementary Fig. S1 and Table S3). The final reconstruction was achieved by merging the three regressions together, with their mean and variance adjusted to be the same as the 1301-1992 nest. The final reconstruction accounts for 63.5% of instrumental Niño3.4 SST variance during 1871-1992 (Fig. 1b).

References

1. McPhaden, M. J., Zebiak, S. E. & Glantz, M. H. ENSO as an integrating concept in earth science. *Science* **314,** 1740–1745 (2006).
2. Deser, C., Alexander, M. A., Xie, S.-P. & Phillips, A. S. Sea surface temperature variability: Patterns and mechanisms. *Annu. Rev. Marine Sci*. **2,** 115–143 (2010).
3. Guilyardi, E. *et al*. Understanding El Niño in ocean–atmosphere General Circulation Models: Progress and challenges. *Bull. Am. Meteorol. Soc.* **90**, 325–340 (2009).
4. Collins, M. *et al*. The impact of global warming on the tropical Pacific Ocean and El Niño. *Nature Geosci.* **3,** 391–397 (2010).
5. Li, J. *et al*. Interdecadal modulation of El Niño amplitude during the past millennium. *Nature Clim. Change* **1,** 114–118 (2011).
6. Stevenson, S. *et al.* Will there be a significant change to El Nino in the 21st Century? *J. Climate* **25,** 2129–2145 (2012).
7. Urban, F. E., Cole, J. E. & Overpeck, J. T. Influence of mean climate change on climate variability from a 155-year tropical Pacific coral record. *Nature* **407,** 989–993 (2000).
8. Cobb, K. M., Charles, C. D., Cheng, H. & Edwards, R. L. El Niño/Southern Oscillation and tropical Pacific climate during the last millennium. *Nature* **424**, 271–276 (2003).
9. Mann, M. E., Bradley, R. S. & Hughes, M. K. Northern Hemisphere temperatures during the past millennium: Inferences, uncertainties, and limitations. *Geophys. Res. Lett.* **26,** 759–762 (1999).

10. Chowdary, J. S. *et al*. Inter-decadal variations in ENSO teleconnection to the Indo-western Pacific for 1870-2007. *J. Climate* **25**, 1722–1744 (2012).

11. Kaplan, A. *et al*. Analyses of global sea surface temperature 1856-1991. *J. Geophys. Res.* **103,** 18567–18589 (1998).

12. Trenberth, K. E. & Stepaniak, D. P. Indices of El Niño evolution. *J. Climate* **14,** 1697–1701 (2001).

13. Ropelewski, C. F. & Jones, P. D. An extension of the Tahiti-Darwin Southern Oscillation Index. *Mon. Wea. Rev.* **115**, 2161–2165 (1987).

14. Mann, M. E. & Lees, J. Robust estimation of background noise and signal detection in climatic time series. *Clim. Change* **33,** 409–445 (1996).

15. Torrence, C. & Compo, G. P. A practical guide to wavelet analysis. *Bull. Amer. Meteor. Soc.* **79,** 61–78 (1998).

16. Ault, T. R. *et al*. Intensified decadal variability in tropical climate during the late 19th century, *Geophys. Res. Lett.* **36,** L08602 (2009).

17. Wittenberg, A. T. Are historical records sufficient to constrain ENSO simulations? *Geophys. Res. Lett.* **36,** L12702 (2009).

18. Gershunov, A., Schneider, N. & Barnett, T. Low-frequency modulation of the ENSO-Indian monsoon rainfall relationship: Signal or noise? *J. Climate* **14**, 2486–2492 (2001).

19. Emile-Geay, J., Cobb, K., Mann, M. & Wittenberg, A. T. Estimating central equatorial Pacific SST variability over the past millennium. Part 2: Reconstructions and uncertainties. *J. Climate* **26,** 2329–2352 (2013).

20. Gershunov, A. & Barnett, T. P. Interdecadal modulation of ENSO teleconnections. *Bull. Am. Meteorol. Soc.* **79,** 2715–2726 (1998).

21. Robock, A. Volcanic eruptions and climate. *Rev. Geophys.* **38,** 191–219 (2000).

22. Adams, J. B., Mann, M. E. & Ammann, C. M. Proxy evidence for an El Niño-like Response to Volcanic Forcing. *Nature* **426,** 274–278 (2003).

23. D'Arrigo, R., Wilson, R. & Tudhope, A. Impact of volcanic forcing on tropical temperatures during the last four centuries. *Nature Geosci.* **2,** 51–56 (2009).

24. Mann, M. E., Cane, M. A., Zebiak, S. E. & Clement, A. Volcanic and solar forcing of the tropical Pacific over the past 1000 years. *J. Climate* **18**, 447–456 (2005).

25. Emile-Geay, J., Seager, R., Cane, M. A., Cook E. R. & Haug, G. H. Volcanoes and ENSO over the past millennium. *J. Climate* **21,** 3134–3148 (2008).

26. McGregor, S. & Timmermann, A. The response of ENSO to explosive volcanic eruptions. *J. Climate* **24,** 2178–2191 (2011).

27. Siebert, L. & Simkin, T. Volcanoes of the world: An illustrated catalog of Holocene volcanoes and their eruptions. Smithsonian Institution, Global Volcanism Program Digital Information Series, GVP-3. (2012).

28. Clement, A. C., Seager, R., Cane, M. A. & Zebiak, S. E. An ocean dynamical thermostat. *J. Climate* **9**, 2190–2196 (1996).

29. Kang, I.-S. Influence of zonal mean flow change on stationary wave fluctuations. *J. Atmos. Sci.* **47**, 141–147 (1990).

30. Palmer, W. C. *Meteorological Drought* U.S. Department of Commerce, Washington D.C. (1965).

Acknowledgements

We thank the researchers who have contributed their tree-ring data for MADA and NADA development, and Dr. Willie Soon for helpful discussions on the records of sunspot number. This research was funded by the National Science Foundation, the National Basic Research Program of China (2012CB955600), the National Oceanic and Atmospheric Administration, the Japan Agency for Marine-Earth Science and Technology, FONDECYT (No.1120965), CONICYT/FONDAP/15110009, CONICET and IAI (CRN2047). This is an International Pacific Research Center/School of Ocean and Earth Science and Technology Contribution (###/####) and a Lamont–Doherty Earth Observatory Contribution (####).

Author contributions

J.L., S.-P.X. and E.R.C. designed the research. J.L., S.-P.X., M.S.M., D.A.C. and N.C.J. analyzed data. J.L., S.-P.X. and N.C.J. wrote the paper. All authors discussed the results and commented on the manuscript.

Additional information

Supplementary information is available in the online version of the paper. Reprints and permissions information is available online at www.nature.com/reprints. Correspondence and requests for materials should be addressed to J.L.

Competing financial interests

The authors declare no competing financial interests.

Figure Captions:

Figure 1 | ENSO reconstruction and verification. a, Spatial correlation field of tree-ring PC1 with global November-January SSTs[11] during 1871-1992. The black box denotes the Niño3.4 region. The shaded letters denote areas where tree rings are sensitive to ENSO (Supplementary Table S2). The black dots indicate site locations mentioned in the text. **b-e,** Comparison of our ENSO reconstruction (blue) with tropical records (red): **b,** NDJ instrumental Niño3.4 index during 1871-2005, **c,** boreal winter (September-February) instrumental SOI during 1867-2005. **d,** Maiana coral $\delta^{18}O$ series[7] during 1841-1994. **e,** Palmyra coral $\delta^{18}O$ series[8] for noncontinuous fractions of the past seven centuries. **f,** The reconstructed NDJ Niño3.4 SSTs over 1301-2005. SST anomalies are relative to the mean of observed SSTs during 1971-2000. The green bold line denotes a 31-yr low-pass filter.

Figure 2 | Modulation of ENSO teleconnections. a, 31-yr running biweight variance for observed (red) and reconstructed (blue) Niño3.4 SSTs. The dashed lines indicate the 95% confidence interval for stochastic variations, based on 10,000 Monte Carlo simulations (Supplementary Methods). **b-d,** 31-yr running correlations of reconstructed Niño3.4 SSTs with tree-ring series from: **b,** Central Asia (blue) and Maritime Continent (red). **c,** Southwest North America (blue) and the Pacific Northwest/TexMex region (red). **d,** South American Altiplano (blue) and northern New Zealand (red). The dashed lines in **b-d** indicate the 0.05 significance level. Vertical shading denotes periods of low ENSO variance.

Figure 3 | ENSO response to large tropical eruptions. a, Superposed Epoch Analysis[22] (SEA) for large tropical eruptions during 1301-2005. Before the SEA, the reconstructed Niño3.4 SSTs were processed using a 9-yr high-pass filter to isolate interannual variability. Error bars denote SST anomalies of one standard deviation at each year. Asterisk (*) denotes anomalies significant at the 0.01 level, based on a two-tailed student's t-test. **b-e**, Composite moisture anomalies associated with **b,** La Niña, **c,** El Niño, **d,** large tropical eruptions at t=0, and **e,** large tropical eruptions at t+1. The El Niño (15) and La Niña (19) events are defined as the NDJ SST anomalies exceeding 0.5°C, using the 9-yr high-pass filtered Niño3.4 index[11] during 1950-2005 (Supplementary Table S6). The number of large tropical eruptions for composite analysis is 22 (Supplementary Table S4). Moisture conditions are indicated by the Palmer Drought Severity Index[30] (PDSI). Positive (negative) anomalies indicate wet (dry) conditions, respectively.

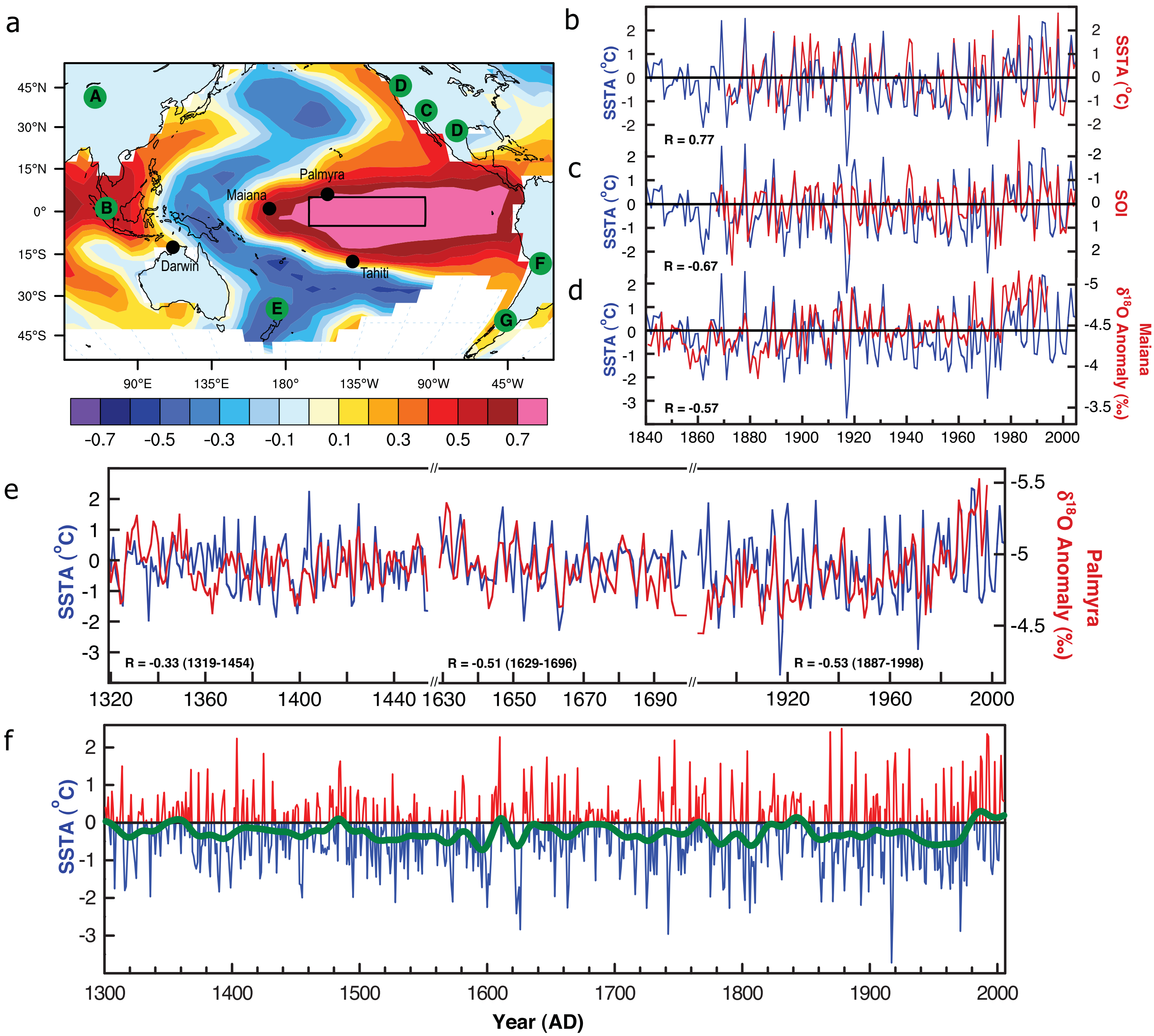
a
b
c
d
e
f
45°N
30°N
15°N
0°
15°S
30°S
45°S
90°E
135°E
180°
135°W
90°W
45°W
Palmyra
Maiana
Darwin
Tahiti
A
B
C
D
E
F
G
-0.7
-0.5
-0.3
-0.1
0.1
0.3
0.5
0.7
SSTA (°C)
SOI
Maiana δ18O Anomaly (‰)
Palmyra δ18O Anomaly (‰)
R = 0.77
R = -0.67
R = -0.57
R = -0.33 (1319-1454)
R = -0.51 (1629-1696)
R = -0.53 (1887-1998)
Year (AD)

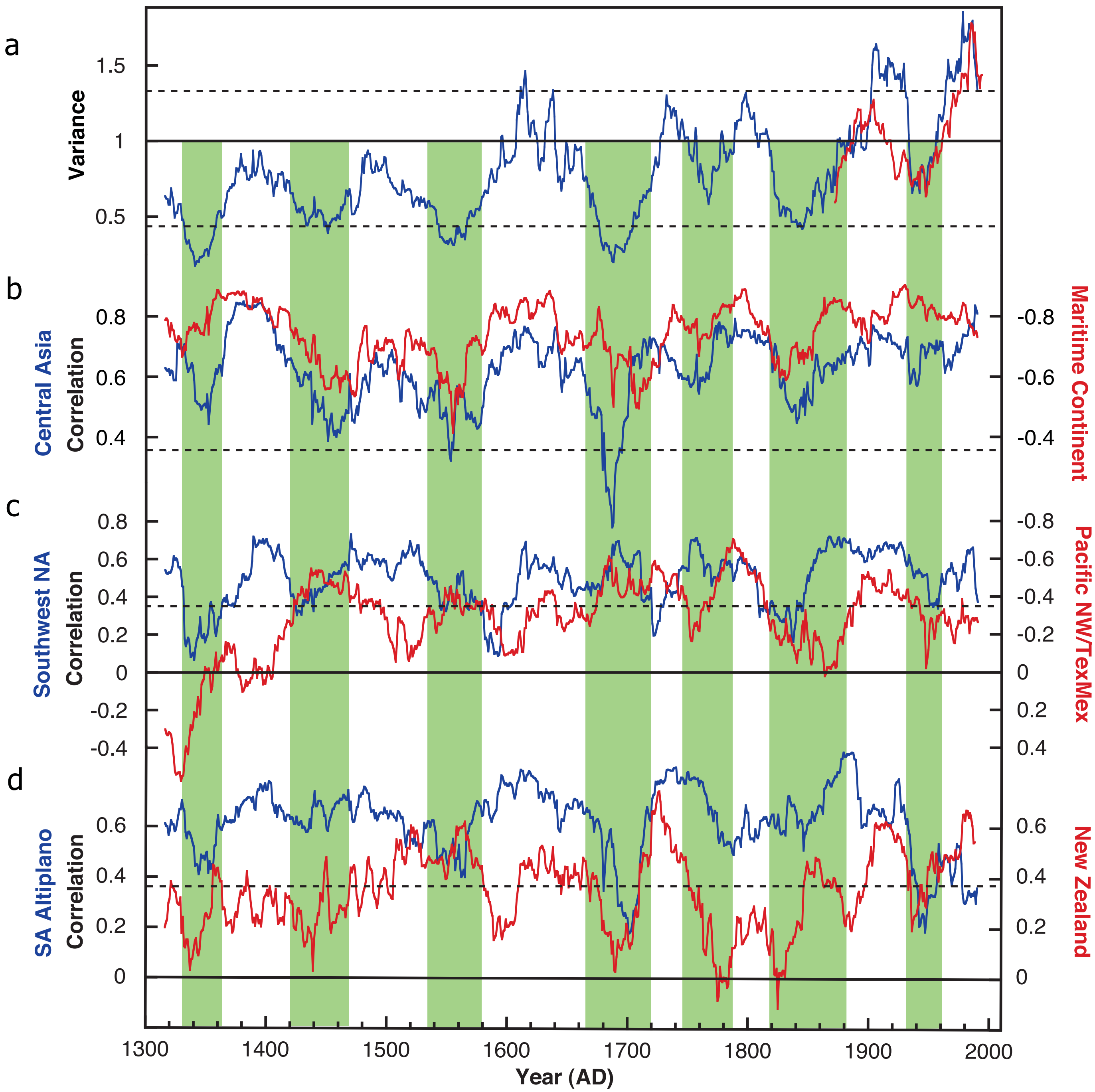

a
Variance
1.5
1
0.5
b
Central Asia
Correlation
0.8
0.6
0.4
Maritime Continent
-0.8
-0.6
-0.4
c
Southwest NA
Correlation
0.8
0.6
0.4
0.2
0
-0.2
-0.4
Pacific NW/TexMex
-0.8
-0.6
-0.4
-0.2
0
0.2
0.4
d
SA Altiplano
Correlation
0.6
0.4
0.2
0
New Zealand
0.6
0.4
0.2
0
1300
1400
1500
1600
1700
1800
1900
2000
Year (AD)

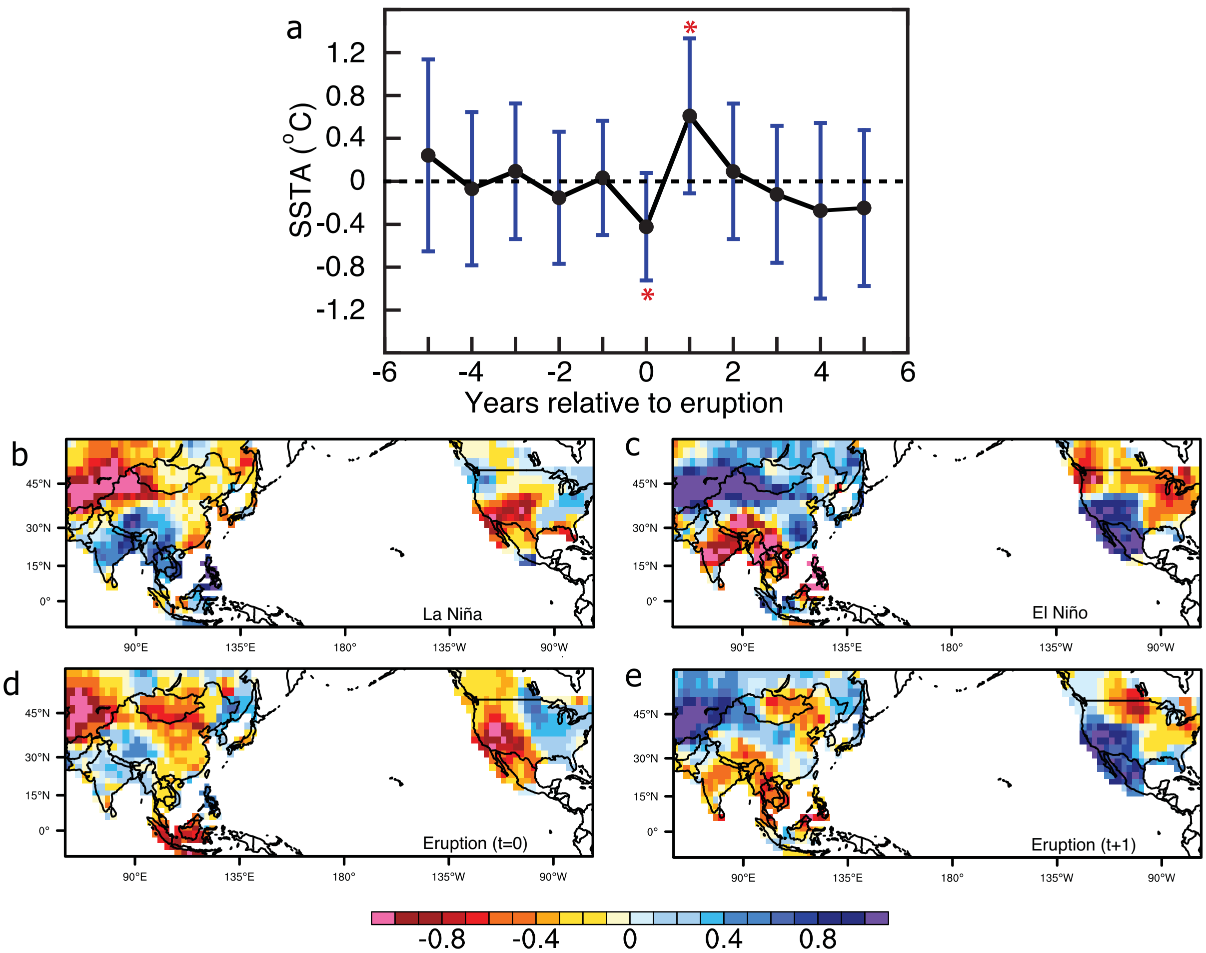
a
SSTA (°C)
Years relative to eruption
b
La Niña
c
El Niño
d
Eruption (t=0)
e
Eruption (t+1)
-0.8
-0.4
0
0.4
0.8